Electron confinement, orbital ordering, and orbital moments in d^0-d^1 oxide heterostructures

Victor Pardo[1,2,*] and Warren E. Pickett[1,†]
[1]*Department of Physics, University of California, Davis, California 95616, USA*
[2]*Departamento de Física Aplicada, Universidade de Santiago de Compostela, E-15782 Santiago de Compostela, Spain*
(Received 14 May 2010; published 17 June 2010)

The $(SrTiO_3)_m/(SrVO_3)_n$ d^0-d^1 multilayer system is studied with first-principles methods through the observed insulator-to-metal transition with increasing thickness of the $SrVO_3$ layer. When correlation effects with reasonable magnitude are included, crystal-field splittings from the structural relaxations together with spin-orbit coupling (SOC) determines the behavior of the electronic and magnetic structures. These confined slabs of $SrVO_3$ prefer $Q_{orb}=(\pi,\pi)$ orbital ordering of $\ell_z=0$ and $\ell_z=-1$ ($j_z=-\frac{1}{2}$) orbitals within the plane, accompanied by $Q_{spin}=(0,0)$ spin order (ferromagnetic alignment). The result is a SOC-driven ferromagnetic Mott insulator. The orbital moment of 0.75 μ_B strongly compensates the spin moment on the $\ell_z=-1$ sublattice. The insulator-metal transition for $n=1\rightarrow 5$ (occurring between $n=4$ and $n=5$) is reproduced. Unlike in the isoelectronic d^0-d^1 TiO_2/VO_2 (rutile structure) system and in spite of some similarities in orbital ordering, no semi-Dirac point [V. Pardo and W. E. Pickett, Phys. Rev. Lett. **102**, 166803 (2009)] is encountered but the insulator-to-metal transition occurs through a different type of unusual phase. For $n=5$ this system is very near (or at) a unique semimetallic state in which the Fermi energy is topologically determined and the Fermi surface consists of identical electron and hole Fermi circles centered at $k=0$. The dispersion consists of what can be regarded as a continuum of radially directed Dirac points, forming a "Dirac circle."

DOI: 10.1103/PhysRevB.81.245117 PACS number(s): 73.20.−r, 75.70.Cn, 79.60.Jv

I. BACKGROUND

Oxide heterostructures with a polar discontinuity across interfaces (IFs) have attracted a great deal of attention recently due to the unusual electronic behavior that can arise.[1,2] It is now becoming evident that heterostructures with nonpolar interfaces can also lead to unanticipated behavior, including low-energy dispersion that is distinct from any previously known system. The specific example is the d^0/d^1 interface system TiO_2/VO_2 that displays a point Fermi surface, from which semi-Dirac dispersion[3] emerges. Semi-Dirac dispersion is characterized by conventional, massive dispersion along one direction in the two-dimensional plane but massless dispersion in the perpendicular direction.

Although reminiscent of graphene, the semi-Dirac system displays its own distinctive low-energy properties.[4] The behavior is actually an electron confinement phenomenon assisted by a particular orbital ordering, and these nanostructures display a peculiar metal-insulator transition[5] as the thickness of the d^1 oxide is increased. In these rutile structured oxides, the metal-insulator transition takes place through an intermediate semi-Dirac point when the thickness is approximately 1 nm, where the system is neither insulating nor conducting and the Fermi surface is pointlike.

Transition metal oxide perovskites with $3d^1$ configuration are known to be on the borderline between metallic and insulating, depending on the relative sizes of several electronic energy scales, including the ratio between the on-site Coulomb repulsion U and the bandwidth W of the d electrons, and the competition between magnetic energies and Jahn-Teller splittings. For small U/W, the material will be metallic, like the correlated metal[6] $SrVO_3$ (SVO). For a large value of the ratio U/W, the system will present a more localized behavior, and a Mott insulator will result, as in $LaTiO_3$ or $YTiO_3$.[7] Other energy scales may also affect, or even determine, the delicate balance.

Multilayers of SVO and $SrTiO_3$ (STO) have been grown on STO substrates by Kim *et al.*[8] and have displayed a transition from the typical insulating behavior of STO to the metallic behavior of SVO as the number of layers of each constituent is increased. Superlattices formed by films with two layers of STO and six layers of SVO [we will denote $(SrTiO_3)_m/(SrVO_3)_n$ (001) oriented multilayers as m/n] already show metallic behavior with a nearly flat resistivity curve with magnitude close to that of SVO. However, from the behavior of the resistivity, it was observed that the 2/3, 2/4, and 2/6 films (increasing SVO thickness) show an insulator-metal transition at temperatures ranging from about 100 K for the 2/6 film to the approximately 230 K of the 2/4 and 2/3 films. It is to be noted also that only two layers of STO are not enough to isolate the SVO slabs, as can be seen from the resistivity data for the 2/3 and 3/3 systems. In fact, the 2/3 system is already semimetallic but four layers of STO are enough to render interactions between neighboring SVO slabs negligible. Five SVO layers are needed to obtain a metallic state, as we show below from our calculations.

In this paper we extend our investigations of d^0-d^1 nanostructures by studying this STO/SVO system, focusing on the differences that the crystal structure, with its specific crystal-field splittings, can cause. We choose the most commonly studied structure, perovskite, with the previously studied nanostructures with rutile crystal structure. We will compare different orbital orderings and magnetic arrangements, and also study how the insulator-to-metal transition occurs with increasing thickness of the d^1 material ($SrVO_3$).

II. COMPUTATIONAL METHODS

Our electronic-structure calculations were performed within density-functional theory[9] using the all-electron, full potential code WIEN2K (Ref. 10) based on the augmented

plane-wave plus local-orbital basis set.[11] The exchange-correlation potential utilized for the structure optimizations was the generalized gradient approximation (GGA) in the Perdew-Burke-Ernzerhof (PBE).[12] To deal with strong correlation effects that are evident in $SrVO_3$ we apply the LSDA+U scheme[13,14] including an on-site U and J (on-site Coulomb repulsion and exchange strengths) for the Ti and V $3d$ states. The values $U=4.5$ eV and $J=0.7$ eV have been used for V to deal properly with correlations in this multilayered structure; these values are comparable to those used in literature for d^1 systems.[15–17] Our calculations show that a larger U, above 5.0 eV, give an incorrect insulating behavior of bulk $SrVO_3$ in cubic structure, hence overestimating electron-electron interactions. Since Ti d states never have any significant occupation, including U or not on Ti $3d$ orbitals has negligible consequence. Spin-orbit coupling (SOC) effects on the valence and conduction states, which are discussed in the last section, have been introduced in a second variational procedure built on the scalar relativistic approximation.

III. TREATING CORRELATION EFFECTS IN BULK $SrVO_3$

We have first performed calculations on bulk SVO to establish the thick $SrVO_3$ limit of these nanostructures. Experimentally, $SrVO_3$ is a ferromagnetic (FM) metal[18] crystallizing in a cubic perovskite structure.[19] No distortion from cubic structure has been observed experimentally, which is consistent to its metallic character; a Mott-insulating d^1 system would be expected to distort due to orbital ordering. Our calculations show that the most stable structure based on GGA exchange correlation (not including on-site Coulomb repulsion effects) is cubic with no distortions. However, a nonmagnetic solution is obtained as a ground state within GGA.

When correlations are introduced by means of the LDA+U method, the most stable structure is slightly distorted. This broken symmetry arises because the LDA+U method tends to promote integer occupations of one of the t_{2g} orbitals (which becomes lower in energy and preferentially occupied).

Calculations were carried out with a tetragonal distortion in bulk $SrVO_3$ and with various values of the on-site Coulomb repulsion U. LDA+U calculations predict two possible orbital configurations: a FM configuration with all the t_{2g} bands equally occupied and an antiferromagnetic (AF) solution with a substantial occupation of the d_{xy} orbital. As U increases above 5 eV, the AF solution is more stable, even for undistorted cubic perovskite, leading to an incorrect AF insulating state. In all ranges of U studied (3–7 eV), a tetragonal distortion is more stable, whereas a simple GGA calculation leads to an undistorted cubic solution, in agreement with experiment. Even in the case of a FM solution, when a U is introduced in the calculations, a tetragonal distortion is obtained as a ground state, in disagreement with experimental observations. Using the correct structure obtained from both experiment and GGA calculations (which agree), the LDA+U method with values of U smaller than 5 eV leads to the correct FM metallic state as ground state.

Within GGA ($U=0$) SVO is a cubic metal, with all the t_{2g} orbitals are equally occupied. Within LDA+U, a tetragonal distortion causes the preferential occupation of the d_{xy} orbital, an insulating state and also an AF ordering to be stabilized, whereas a cubic FM metallic state is observed experimentally. This is the case also when LDA+U is applied for the structure relaxed with GGA. For this reason, throughout the paper, we will use for structure optimizations of these multilayers including such a moderately correlated compound, the GGA-PBE functional.[12] With the structure thus determined, we use the LDA+U method for the calculations of the electronic and magnetic structures, and energy differences. In bulk SVO this procedure properly results in a FM half metal with 1 μ_B/V atom.

IV. GENERAL CONSIDERATIONS

$SrVO_3$ has a lattice parameter of 3.84 Å (Ref. 19) while the lattice parameter of STO is 3.90 Å.[20] Since most of these superlattices are grown on a $SrTiO_3$ substrate, for closest comparison with experimental data we fix the a lattice parameter to be the STO lattice parameter. However, we use the GGA-PBE exchange-correlation potential to optimize the superlattice c parameter and also the internal coordinates of all the atoms by a force minimization together with a total-energy minimization.

Since the IF between SVO and STO has no polar discontinuity, the distortions introduced at the interface between the two oxides by the nanostructuring can be understood as first, strain due to the lattice-parameter mismatch (1.5%) and second, to charge imbalance within the V t_{2g} orbitals. Of course, any IF between two different materials is not strictly nonpolar, locally. The sense in which this terminology is used here is that, using formal charges, alternating layers on either side of the IF (strictly, far enough from the IF) have similar charges. $V^{4+}O_2^{2-}$ and $Ti^{4+}O_2^{2-}$ clearly satisfy this criterion. Thus, in this system no ionic charge compensation effects of the sort that are so interesting in $LaAlO_3/SrTiO_3$ nanostructures are present.[1,21–26]

We compare results for m/n multilayers with $m=4$ layers of STO (about 1.6 nm thickness) sandwiching an SVO layer with variable thickness from 1 to 5 layers of SVO (0.4 to 2.0 nm) because we find four layers of STO sufficient to isolate the SVO slabs to give two-dimensional behavior (negligible k_z dispersion in the band structure). We analyze the evolution of the electronic structure for increasing thickness of SVO slabs (n from 1 to 5).

A. d^1 V ion in an octahedral environment

One common feature within the SVO sublayer for all thicknesses we have studied is that the V octahedral environment, especially at the IF, will be tetrahedrally distorted from its cubic symmetry in the bulk. It was noted above that such a distortion, treated fully (i.e., including structural relaxation) within the LDA+U method for reasonable values of U, produces an (incorrect) AF insulator state for bulk SVO. In the case of the multilayers, our relaxation of the c lattice param-

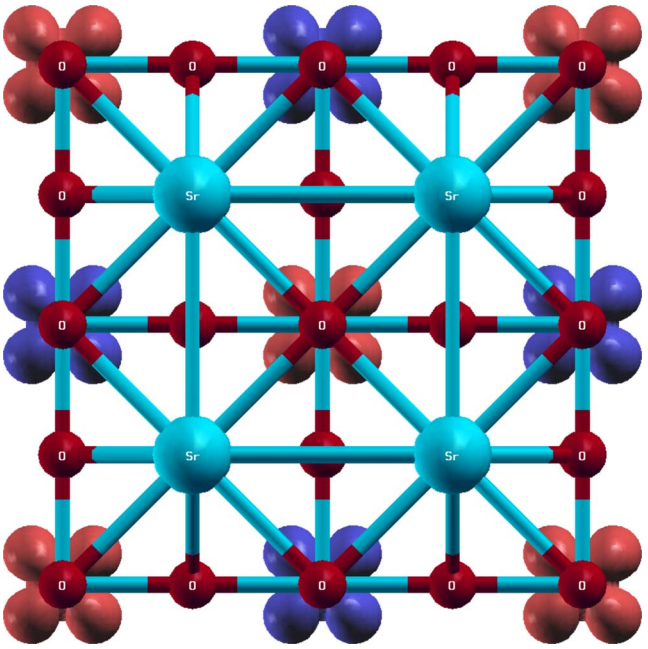

FIG. 1. (Color online) Spin density isosurface of the $n=2$ system at 0.8 e/Å^3. Shown is a top view of the x-y plane in the planar AF Mott insulator state, which is the most stable only at larger values of U. The d_{xy} orbital is occupied on each V ion. Different colors indicate different spin directions.

eter and atomic positions will lead to values of the interplane V-V distance somewhat smaller than the in-plane value. The simplest scenario would be that the multilayer structuring of SVO on an STO substrate will produce a tetragonal distortion of the oxygen octahedra around the V cations. This c-axis contraction of the octahedra leads to a preferred occupation of the d_{xy} orbital. If d_{xy} orbitals are occupied on all atoms in a layer, a small enough bandwidth or strong enough intra-atomic interaction U will give AF ordering by superexchange. This effect is observed experimentally in similar multilayer systems with the d^1 compound being a Mott insulator such as $LaTiO_3$.[27]

A more realistic picture must allow for the likelihood that the degenerate d_{xz},d_{yz} orbitals will have a narrower bandwidth in the x-y plane, and correlation effects may favor occupation of some combination of these orbitals. Even though small, spin-orbit coupling breaks this degeneracy and specifies a favored combination. The actual occupation will depend on several factors. First of all is the tetragonal crystal-field splitting of the t_{2g} orbitals. In all cases we study, the xy on-site energy is lower due to in-plane stretching imposed by the STO substrate. Second, the x-y plane bandwidths of d_{xy} and d_{xz},d_{yz} bands are very different, and will depend on orbital order. Third, the orbital order is closely tied to the magnetic configuration of the system. The simplest possibility (above), with all the electrons in a d_{xy} orbital, leads to AF order (this orbital pattern can be seen in Fig. 1), whereas we find that occupying d_{xz},d_{yz} orbitals favors FM order.

B. Structural relaxation: Strain effects

The structural distortion as n increases can be described in terms of lattice strain along the c axis. Relaxing the c-axis value (and also the internal atomic positions) yields the results provided in Table I. For understanding the structural distortions, we can define four different distances along the c axis (within the plane they are constrained by the STO lattice parameter 3.905 Å): the V-V distance, the V-Ti distance across the IF, the Ti-Ti distance, and finally the average c lattice parameter. We find that the Ti-Ti distance hardly changes and also the V-Ti distance variation is minor. However, the V-V distance grows toward a limiting value as the number of SVO layers increases. Both V-V and Ti-Ti interlayer distances presented in the table vary only by ±0.01 Å for the various layers within each n/m system.

TABLE I. Interlayer distances (Å) between metal cations for the various n/m configurations under study. The important distances to describe the structure are Ti-Ti, Ti-V (across the interface), V-V, and the average c parameter. The Ti-Ti separations and V-V separations, for each heterostructure are uniform to within 0.01 Å.

	Ti-Ti	V-Ti	V-V	c_{av}
4/1	3.97	3.92		3.95
4/2	3.95	3.90	3.79	3.91
4/3	3.95	3.91	3.83	3.91
4/4	3.98	3.94	3.86	3.92
4/5	3.98	3.93	3.87	3.92

C. Band lineups; intralayer supercells

Some general features should be established. Due to the alignment of the $SrVO_3$ Fermi level (or gap) within the $SrTiO_3$ gap between filled O $2p$ states and empty Ti $3d$ states, there is a 2.5 eV energy window which contains only the V d bands that are of interest for us. The oxygen $2p$ bands lie below the V d bands. We note especially that we have used laterally enlarged, $c(2\times2)$ superstructures to allow the possibility (or likelihood) of AF spin alignment as well as FM, and various orbital ordering patterns as well. The ground states we obtain and analyze are all lower in energy than any that would have been found in primitive $p(1\times1)$ cells.

D. Spin-orbit coupling

SOC in the V atom usually produces minor effects, except for those which depend entirely on it (such as magnetocrystalline anisotropy). We find here however, irrespective of the number of VO_2 layers, that SOC in conjunction with correlation effects (the on-site repulsion U) completely alter the ground state that we obtain.

It has long been known that the t_{2g} subshell provides a representation for $\ell=1$ (not $\ell=2$) orbital moments.[28–32] The m_ℓ states are $d_0=d_{xy}$ and $d_\pm=d_{xz}\pm id_{yz}$. SOC splits these, with $d_-(j_z=-\frac{1}{2})$ lying lower. This viewpoint is not common because the orbital moments are typically quenched by mixing with neighboring orbitals. Fairly recently several cases have come to light in which t_{2g} orbital moments can be quenched[33] by structure-induced or spontaneous symmetry lowering, or even in a $5d$ system an orbital moment can

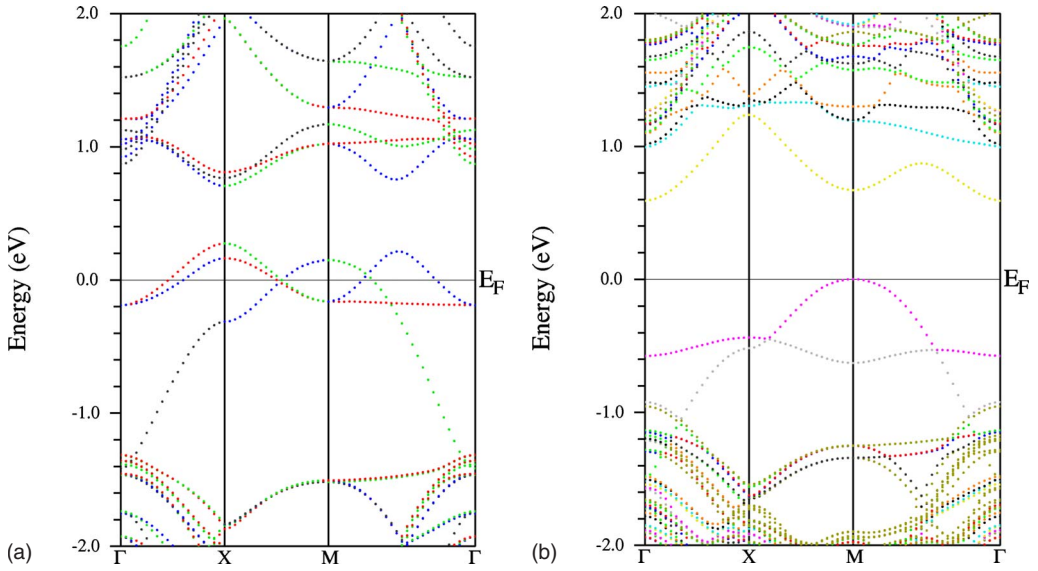

FIG. 2. (Color online) Majority spin LDA+U band structure of the $n=1$ system without (left panel) and with spin-orbit coupling (right panel) included. A SOC-driven FM Mott insulator regime occurs at this very small SVO thickness: the introduction of SOC breaks the d_{xz}, d_{yz} symmetry, and LDA+U splits the d_- (down) and d_+ states (up), opening the gap. The lower and upper Hubbard bands lie at −0.5 eV and 1.3 eV, respectively.

compensate a spin moment and prevent orbital ordering.[34] The calculations presented here provide an additional example of the importance of SOC in 3d systems.

The strain in the slabs we study breaks the t_{2g} symmetry, with d_{xy} lying lower. Strong magnetocrystalline anisotropy favors the magnetization along the c axis (by 130 meV/V compared to an in-plane orientation), making this the quantization axis. Then one can expect competition between occupation of the d_- and d_{xy} orbitals in a d^1 ion, with kinetic energy (bandwidth and band placement) being a determining factor. The energy gain, and thus the large magnetocrystalline anisotropy, is related (see following sections) to the formation of a large orbital moment 0.75 μ_B along the z axis when the d_- orbital is occupied. Since the spin moment is reduced somewhat from its atomic value of 1 μ_B by hybridization, the net magnetic moment on such an ion can be quite small.

In the next section we show that an alternating orbitally ordered (AOO) state, with half the electrons in a d_{xy} orbital and the other sublattice in a $d_\pm$ orbital, arises and leads to FM spin alignment. The AF solution becomes favored only at unphysically large values of U (above 5–6 eV). In the reasonable range of values of U, this AOO state is energetically favored for several SVO slab thicknesses. This AOO, Mott-insulating FM state competes and overcomes the Mott-insulating AF state, which has all the electrons in xy orbitals. Unexpectedly, when SOC is included, the alternating orbital ordering produces an FM Mott-insulating state at small $SrVO_3$ thicknesses, below 2 nm, and for realistic values of U for this multilayered system. It is instructive to follow the behavior through the insulator-to-metal transition with SVO thickness.

V. EVOLUTION OF THE ELECTRONIC STRUCTURE

A. $n=1$ confined layer of $SrVO_3$

When a single layer of SVO is confined by insulating STO, the resulting strain lowers the d_{xy} orbital energy and it should be expected that a candidate ground state is d_{xy} "orbitally ordered" AF insulator due to superexchange. Indeed this Néel state can be obtained in our calculations for the moderate range of U that is relevant. The coupling arises through $dd\pi$-type hopping between d_{xy} orbitals in the plane (see Fig. 1) as expected from Goodenough-Kanamori-Anderson rules.[35] However, the AOO phase with FM spin alignment was also obtained and it is lower in energy by 4 meV/V. The two sublattices lead to distinct sets of bands, as easily seen from the left panel of Fig. 2. The d_{xy} band has the familiar square-lattice shape (distorted somewhat by second neighbor coupling) and is 1.5 eV wide. The d_{xz}-d_{yz} bands are much narrower (0.25 eV) because there is only $dd\pi$ coupling. The centroid of the latter pair lies about 0.5 eV above that of the d_{xy} band, providing the magnitude of the splitting of the t_{2g} by strain. The system is metallic, with all three bands leading to Fermi surfaces.

The picture is completely changed by SOC. Figure 2 compares the majority-spin band structure of the FM AOO state, first without SOC, then with SOC included. SOC has no effect on the d_{xy} ($\ell_z=0$) band. However, SOC breaks the symmetry of the $\ell_z=\pm 1$ doublet and the narrow bandwidth (0.25 eV) compared to the value of U results in a Mott-insulating type of splitting of the d_- and d_+ bands, by roughly $\pm U$. The SOC-driven symmetry lowering is leveraged by the strong on-site interaction. The result is an AOO FM Mott insulator with a gap of 0.6 eV. This d_- orbital acquires a large orbital moment of about 0.75 μ_B, strongly compensating the

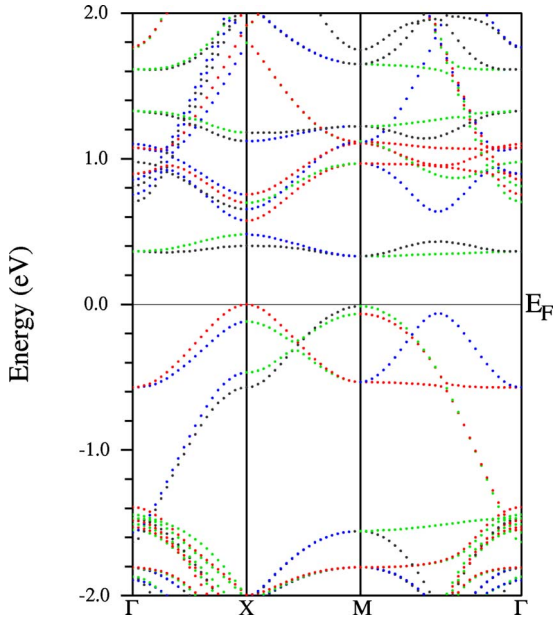

FIG. 3. (Color online) LDA+U band structure (without SOC) of the 4/2 system (U=4.5 eV). A Mott-insulator regime occurs at this thickness of two SVO monolayers.

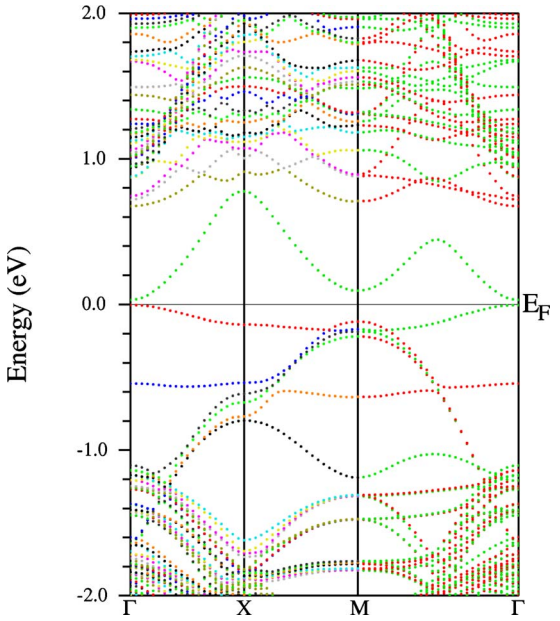

FIG. 4. (Color online) Band structure of the 4/3 system for U =4.5 eV with spin-orbit coupling. The minority-spin state would be equivalent in this AF ground state. A very small gap insulator is obtained, on the verge of a metal-insulator transition. A metal is actually obtained at small U (below 4 eV).

spin moment. This motif of FM AOO V orbitals will recur for thicker SVO slabs.

B. n=2 $SrVO_3$ layers

The bands near the gap for the two SVO layer slab are displayed in Fig. 3 without SOC included, to illustrate that for two layers there is already a band gap without SOC, produced by interlayer coupling of d_{xz},d_{yz} states. However, SOC produces the same orbital ordering and intralayer FM alignment as for n=1 and the layers are also spin aligned to give an overall FM AOO Mott-insulating state. Comparing the total energy for the d_{xy} AF state with the more stable FM state, the energy difference is found to be large, 76 meV/V. This energy difference includes the in-plane energy gain as for n=1 and the larger interplane stabilization due to a large $dd\sigma$ coupling between d_{-} orbitals.

C. n=3 $SrVO_3$ layers

As mentioned earlier, structural relaxation was always carried out using only the GGA exchange-correlation functional. We note that for this n=3 case GGA calculations give an AF interplane coupling (up/down/up) of FM layers. We carried out the structural relaxations in this magnetic structure; however, the type of magnetic order is not expected to affect the relaxation appreciably.

Returning to the LDA+U calculations to evaluate spin and orbital orders, the ground state is FM overall (up/up/up) with AOO within the plane and a metallic band structure. As for n=1 and n=2, in-plane AF ordering with all d_{xy} orbitals occupied can be obtained but is energetically higher than the FM AOO state. In this case, we can compare the total energies of two configurations with the same in-plane orbital ordering, but different interlayer AOO alignment, AAA (like orbitals aligned along the c axis) or ABA. The AAA configuration is more stable by 6 meV/V, giving an idea of the strength of the interlayer coupling.

SOC again results in the same intralayer AOO FM state, however in this case there is an extremely small gap at Γ, visible in Fig. 4. It differs from the n=2 system (and is similar to the n=1 system) in having a gap only when SOC in included (breaking the $d_{\pm}$ degeneracy that otherwise leaves half (or partially) filled bands).

D. n=4 $SrVO_3$ layers

The band structure of the n=4 system, which has the same AOO (Fig. 5) FM Mott-insulating ground state, is shown neglecting SOC in Fig. 6 to show that SOC is not necessary to produce a gap (as for n=2), although it does change the band structure. The four nearly degenerate d_{xy} bands with their simple square-lattice shape lie in the −1.6 to −0.1 eV range, interlayer coupling is very small for these d_{xy} orbitals. The four band pairs for the d_{xz},d_{yz} orbitals correspond to linear combinations of similarly shaped bands for each of the four layers. The band dispersion decreases from 0.7 eV for the lowest band to zero for the highest (unoccupied) bands. By using a simple tight-binding model with interplane coupling, the band ordering and hence the occupation of the bands is readily reproduced.

E. n=5 $SrVO_3$ layers

For n=5 several orbital orderings can be obtained and their energies compared. Of the solutions we studied, again the AOO FM layers, spin aligned between layers (globally FM) is again the ground state. Tetragonal strain and SOC

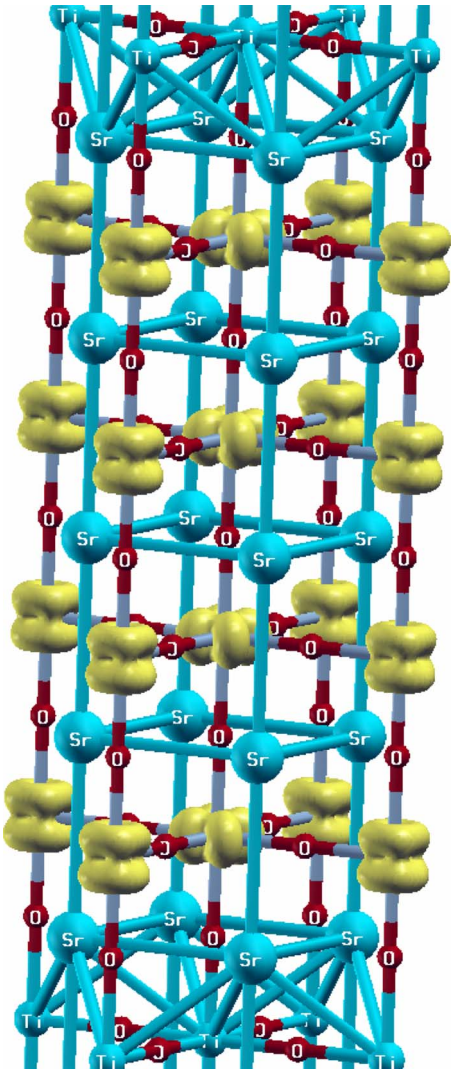

FIG. 5. (Color online) Spin density isosurface of the $n=4$ system ($U=4.5$ eV) of the majority-spin electrons of this FM insulating solution. The in-plane alternating orbital ordering d_{xy} and d_{-} orbitals is apparent, and also the interlayer orbital configuration. The ferro-orbital occupation along the z axis is stabilized by the interaction between V $d_{xz\pm iyz}$ orbitals in this FM ground state.

result in the same AOO arrangement and corresponding identifiable bands, which are shown in Fig. 7. The five d_{xy} bands have a total splitting no more than 0.4 eV and are completely filled. The five d_{-} bands, each with small bandwidth, cover a range of 1.4 eV. The lower two (−1.4 to −0.9 eV) mix with the O $2p$ bands and are not as obvious as the upper three bands.

The distinction for $n=5$ is that the uppermost d_{-} band is not fully occupied but overlaps by 0.2 eV a conduction band that dips below the d_{-} at the Γ point and leads to a semimetal. The insulator-to-metal transition has occurred between $n=4$ and $n=5$, very similar to the transition observed by Kim *et al.*[8] in their SVO/STO multilayers. Unlike the VO_2/TiO_2 system where the transition proceeds through a point Fermi surface, semi-Dirac phase,[3–5] this transition appears to occur in the classic fashion of band overlap. The strong effects of tetragonal strain (symmetry breaking) and SOC (further symmetry breaking) are finally overcome by the increasing delocalization across the SVO slab as the quantum confinement effects are eroded.

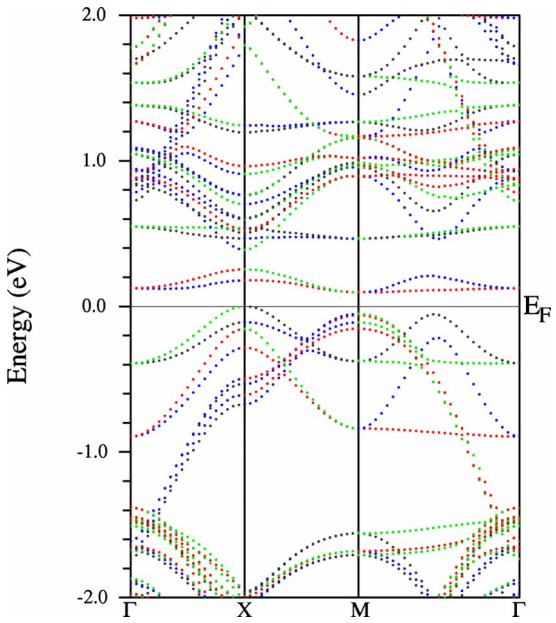

FIG. 6. (Color online) Majority spin band structure of the $n=4$ system ($U=4.5$ eV) of this FM half-metallic, orbitally ordered ground state. The four characteristic, nearly degenerate d_{xy} bands lie in the −1.6 to −0.2 eV range. There is ferro-orbital ordering between planes. The interlayer coupling splits the d_{-} bands by 0.2–0.3 eV.

VI. TRANSITION THROUGH A SINGULAR FERMI SURFACE

A very unconventional insulator-to-metal transition nearly occurs at the $n=5$ thickness and might actually occur for somewhat different value of intra-atomic repulsion U or different value of strain. If some small change lifted the conduction band at the M point in Fig. 7 above the Fermi level (it overlaps only slightly as it is) and if the overlapping valence and conduction bands at Γ are in the (small k) quadratic limit so their constant energy surfaces are circles, then the equality of electron and hole density leads to *coinciding* electron and hole Fermi surfaces. The "Fermi surface" is actually two identical electron and hole Fermi lines, the Fermi surface has a boundary but no area. The bands near the Fermi energy, given in the simplest model by

$$\epsilon_k = \pm v(|\vec{k}| - k_F) \quad (1)$$

are presented in Fig. 8, where these linearly dispersing bands are shown. With doping, the electron and hole surfaces (lines since this is two dimensions) separate, leaving an annulus that contains electrons if electron doped or holes if it is hole doped. It is thus easy to understand how the annulus vanished as the doping level vanishes. The situation is in fact a continuum of radial Dirac points. Conversely, it presents the limit of a semi-Dirac point[3,4] when the effective mass diverges.

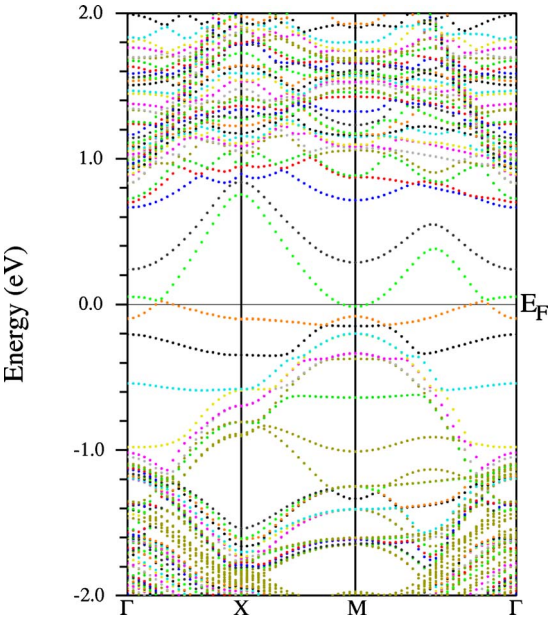

FIG. 7. (Color online) Band structure of the 4/5 system (U =4.5 eV) of the majority spin of this FM half-metallic state. There is orbital ordering in plane and ferro-orbital ordering between layers, as for thinner $SrVO_3$ slabs. However, with the added bands, the interlayer coupling is no longer large enough to open a gap, leaving a semimetallic state with band overlap at Γ.

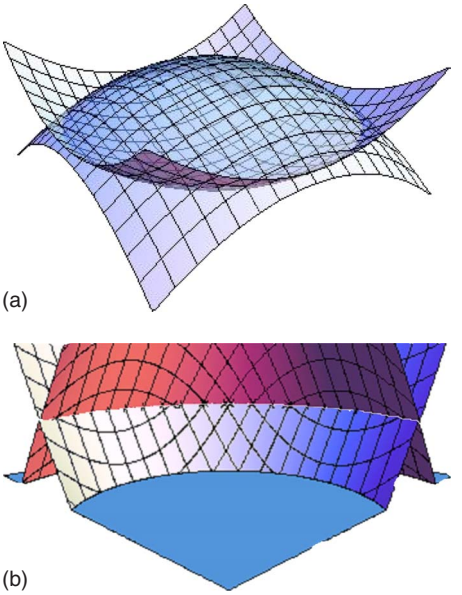

FIG. 8. (Color online) The model depicted represents the two bands closest to the Fermi level for the n=5 system displayed in Fig. 7. Two (locally) linearly dispersive bands in the form $\epsilon_k = \pm v||k|-k_F|$ come together (top panel) forming a continuous circle of Dirac points, i.e., a "Dirac circle". In the lower panel, only one quadrant is shown to allow the Dirac crossing of bands to be seen.

From Fig. 7, it is clear that (with the conduction band at M out of the picture) the positioning of the Fermi level at the band crossing *point* is topologically determined: only for precisely that Fermi level is an integral number of bands occupied, which is exactly what is required to occupy the V 3d electrons. The lowering of the symmetry of the eigenstates off of the symmetry directions (corresponding to some subgroup of the group of the symmetric k point) may lead to coupling of the bands and the opening of a gap away from the X or M points (or both). In this case, one is left with four (respectively, eight) semi-Dirac points along symmetry lines.

However, it may occur that the bands have different symmetry throughout the Brillouin zone in which case no gap opens. The simplest example is even and odd symmetry under z reflection, d_{xy} states, for example, being even and d_{xz}, d_{yz} states being odd. This is the case in which this Dirac continuum of points may arise.

VII. SUMMARY

We have analyzed the transition from insulator to metal in the electronic structure of multilayers $(SrTiO_3)_4/(SrVO_3)_n$, with n varying from 1 to 5. The transition is observed to occur between n=4 and n=5. The origin of the observed changes is surprisingly intricate, with tetragonal strain and spin-orbit coupling (each with an associated symmetry breaking) leveraging strong-interaction effects modeled by the LDA+U approach. The effects of quantum confinement finally determine the conduction character. Insulating behavior with a peculiar alternating orbital ordering within each V layer and FM magnetic order results from a ferromagnetic Mott-insulating state for n=4 or less. Ferromagnetic Mott insulators are rare and these results indicate how this kind may be achieved (even designed) in oxide nanostructures. The FM insulator-to-FM metal transition finally results from band overlap as quantum confinement effects decrease. This system is very close to, if not at, an unusual semimetal state for n=5 in which the Fermi surface is topologically determined and consists of two degenerate electron and hole circles around the k=0 point.

ACKNOWLEDGMENTS

This project was supported by DOE under Grant No. DE-FG02-04ER46111 and through interactions with the Predictive Capability for Strongly Correlated Systems team of the Computational Materials Science Network.

*victor.pardo@usc.es
†wepickett@ucdavis.edu

[1] N. Nakagawa, H. Y. Hwang, and D. A. Muller, Nature Mater. **5**, 204 (2006).
[2] R. Pentcheva and W. E. Pickett, J. Phys.: Condens. Matter **22**, 043001 (2010).
[3] V. Pardo and W. E. Pickett, Phys. Rev. Lett. **102**, 166803 (2009).
[4] S. Banerjee, R. R. P. Singh, V. Pardo, and W. E. Pickett, Phys. Rev. Lett. **103**, 016402 (2009).
[5] V. Pardo and W. E. Pickett, Phys. Rev. B **81**, 035111 (2010).
[6] P. Dougier, J. C. C. Fan, and J. B. Goodenough, J. Solid State Chem. **14**, 247 (1975).
[7] E. Pavarini, S. Biermann, A. Poteryaev, A. I. Lichtenstein, A. Georges, and O. K. Andersen, Phys. Rev. Lett. **92**, 176403 (2004).
[8] D. H. Kim, D. W. Kim, B. S. Kang, T. W. Noh, D. R. Lee, K. B. Lee, and S. J. Lee, Solid State Commun. **114**, 473 (2000).
[9] P. Hohenberg and W. Kohn, Phys. Rev. **136**, B864 (1964).
[10] K. Schwarz and P. Blaha, Comput. Mater. Sci. **28**, 259 (2003).
[11] E. Sjöstedt, L. Nördstrom, and D. J. Singh, Solid State Commun. **114**, 15 (2000).
[12] J. P. Perdew, K. Burke, and M. Ernzerhof, Phys. Rev. Lett. **77**, 3865 (1996).
[13] V. I. Anisimov, J. Zaanen, and O. K. Andersen, Phys. Rev. B **44**, 943 (1991).
[14] E. R. Ylvisaker, W. E. Pickett, and K. Koepernik, Phys. Rev. B **79**, 035103 (2009).
[15] S. Biermann, A. Poteryaev, A. I. Lichtenstein, and A. Georges, Phys. Rev. Lett. **94**, 026404 (2005).
[16] J. M. Tomczak and S. Biermann, J. Phys.: Condens. Matter **19**, 365206 (2007).
[17] M. W. Haverkort *et al.*, Phys. Rev. Lett. **95**, 196404 (2005).
[18] I. H. Inoue, O. Goto, H. Makino, N. E. Hussey, and M. Ishikawa, Phys. Rev. B **58**, 4372 (1998).
[19] Y. C. Lan, X. L. Chen, and M. He, J. Alloys Compd. **354**, 95 (2003).
[20] M. Dawber, C. Lichtensteiger, M. Cantoni, M. Veithen, P. Ghosez, K. Johnston, K. M. Rabe, and J. M. Triscone, Phys. Rev. Lett. **95**, 177601 (2005).
[21] A. Ohtomo and H. Y. Hwang, Nature (London) **427**, 423 (2004).
[22] R. Pentcheva and W. E. Pickett, Phys. Rev. B **78**, 205106 (2008).
[23] P. R. Willmott *et al.*, Phys. Rev. Lett. **99**, 155502 (2007).
[24] W. Siemons, G. Koster, H. Yamamoto, W. A. Harrison, G. Lucovsky, T. H. Geballe, D. H. A. Blank, and M. R. Beasley, Phys. Rev. Lett. **98**, 196802 (2007).
[25] M. S. Park, S. H. Rhim, and A. J. Freeman, Phys. Rev. B **74**, 205416 (2006).
[26] R. Pentcheva and W. E. Pickett, Phys. Rev. B **74**, 035112 (2006).
[27] S. S. A. Seo, M. J. Han, G. W. J. Hassink, W. S. Choi, S. J. Moon, J. S. Kim, T. Susaki, Y. S. Lee, J. Yu, C. Bernhard, H. Y. Hwang, G. Rijnders, D. H. A. Blank, B. Keimer, and T. W. Noh, Phys. Rev. Lett. **104**, 036401 (2010).
[28] A. Abragam and B. Bleaney, *Electron Paramagnetic Resonance of Transition Ions* (Clarendon Press, Oxford, 1970).
[29] K. W. H. Stevens, Proc. R. Soc. London, Ser. A **219**, 542 (1953).
[30] J. B. Goodenough, Phys. Rev. **171**, 466 (1968).
[31] C. Lacroix, J. Phys. C **13**, 5125 (1980).
[32] W. E. Pickett and H. Eschrig, J. Phys.: Condens. Matter **19**, 315203 (2007).
[33] G. Khaliullin and S. Maekawa, Phys. Rev. Lett. **85**, 3950 (2000).
[34] K. W. Lee and W. E. Pickett, EPL **80**, 37008 (2007).
[35] J. B. Goodenough, *Magnetism and the Chemical Bond* (IEEE Press, New York, 2001).